e-PS, 2005, **2**, 31-37
ISSN: 1581-9280

www.e-PreservationScience.org
www.Morana-rtd.com

e-PRESERVATIONScience
published by MORANA RTD d.o.o.

FULL PAPER

REVIEW

SHORT COMMUNICATION

MEASURING CRYSTALLINITY OF LASER CLEANED SILK BY X-RAY DIFFRACTION

CRAIG J. KENNEDY[1*], KARIN VON LERBER[2], TIM J. WESS[1]

1 Structural Biophysics Group, School of Optometry and Vision Sciences, Cardiff University, Redwood Building, King Edward VII Avenue, Cardiff, Wales, CF10 3NB, UK

2 Prevart GmbH – Textile Conservation, Oberseenerstr. 93, CH-8405 Winterthur, Switzerland

*corresponding author: kennedyc1@cardiff.ac.uk

received: 24.11.2005
accepted: 07.12.2005

key words: Silk, crystallinity, X-ray diffraction, crystal size, Scherrer

Abstract

We present an effective and sensitive method of analyzing the condition of silk following laser cleaning. New silk samples were analysed; two sets were soiled with carbon black before laser cleaning and two sets were left unsoiled. Samples were exposed to laser cleaning at a wavelength of 532 nm and a fluence of 1.5 J/cm^2 for 4, 16 and 64 pulses. Two sample sets were also treated at fluence levels of 0.5, 1.0 and 4.2 J/cm^2 to assess the effects of fluence on the silk structure. Wide angle X-ray diffraction was carried out using the NanoSTAR facility at Cardiff University. Using the main equatorial reflections from silk the crystallinity of the samples was calculated. Upon laser cleaning at 1.5 J/cm^2, the silk displayed a reduced level of crystallinity as the number of pulses increased, with soiled silks displaying a greater crystallinity loss than unsoiled silks. Coupled with this, the crystal size, as analysed using the Scherrer formula, was shown to increase as the crystallinity reduced. The effects of fluence on the sample crystallinity was less obvious: samples treated at 0.5 J/cm^2 displayed an intrinsically higher crystallinity than all other samples, but there was no progressive loss of crystallinity with increasing fluence level as may have been anticipated.

1. Introduction

Removing surface particulates from historical materials is an important aspect of conservation. Over time historical artifacts such as documents, textiles and sculptures become exposed to the effects of environmental pollution, which has sharply increased over the last 100 years. Many conventional cleaning techniques include the use of water, solvents such as isopropanol and ethanol, or mechanical action (brushing, sponges, erasors). Techniques such as these may alter the aesthetic or mechanical properties of the material.

Lasers have provided the potential for contact-less, solvent-free cleaning of materials. Laser cleaning has been developed and used extensively in the cleaning of sculptures and buildings[1-5]. In recent

years however the use of laser cleaning biologically based materials has been investigated[6-11]. The effects of laser cleaning on silk[12] have been less extensively investigated than the effects on, for example, paper.

Materials such as paper, parchment and silk are made up of fibrous biopolymers (cellulose, collagen and fibroin respectively) that retain many of the structural characteristics that made them biologically useful. These biopolymers provide mechanical strength to their native systems; this strength derives from the discrete structural hierarchies that exist on the molecular, nanoscopic and mesoscopic levels. Molecules pack together to form fibrils or structural modules that are the fundamental providers of strength. The bonds that retain the molecular structures of these biomaterials are relatively weak; cellulose[13], collagen[14] and silk[15] are susceptible to damage induced by the use of lasers at lower energy levels than stone or marble[16]. Should the energy of the lasers disrupt the molecular bonds, the overall strength of the material in question may be compromised.

The hierarchical organisation of fibrous biopolymers occurs on different length scales. X-ray wide angle (WAXS), small angle (SAXS) and ultra-small angle (USAXS) scattering techniques can be used to study the sample characteristics from the unit cell level (Ångstroms) to the mesoscopic level (nm), to the light scattering level (microns) respectively. These techniques have a distinct advantage over other biophysical methods (i.e. electron microscopy) in that minimal sample preparation is required; subsequently, more information is available regarding the natural state of the material. In this study WAXS is employed which provides information regarding the small-scale structure of silk, inter-molecular and fibrillar interactions.

A number of X-ray diffraction studies of spider silk have been conducted[17,18], as a large quantity is readily available due to the “forced silking” technique[19], or silkworms. Silks from a number of spider species display a β-poly(L-alanine) structure, as observed by X-ray microdiffraction[20]. Silk from orb weaving spiders such as *Nephila clavipes* or from the wild silkworm (*Tussah* silk) also display this structure. The domesticated silkworm *Bombyx Mori* produces silk with a crystalline β-poly(alanylglycine) structure[17].

2. Materials and Methods

2.1 Silk Samples

The samples used here were those used by von Lerber et al[12]. Four sets of new, undyed silks were used. Two sets were left unsoiled (sets 1 & 2), and two sets were soiled with carbon dust (sets 3 & 4). Silk samples were treated with an Nd:YAG laser at a wavelength of 532 nm and a fluence (energy) level of 1.5 J/cm^2, with 4, 16 or 64 pulses. The laser used operates with a pulse duration of 9 ns, a repetition rate of 500 Hz, and a maximum energy of 2.5 mJ. The computerised system allowed for reproducible treatment techniques. An even distribution of fluence over the whole sample surface was achieved using the overlap of the Gaussian beam distribution.

To assess the effect of fluence level, sample sets 2 and 4 were used. They were laser cleaned as described above, but at fluence levels of 0.5, 1 and 4.2 J/cm^2.

2.2 X-ray Diffraction

Samples were mounted in the sample chamber of the NanoSTAR (Bruker AXS, Germany) facility at Cardiff University and placed under vacuum. The data collection procedure used followed that described in detail by Wess *et al*[22].

The NanoSTAR facility is an in-house lab-based X-ray diffraction system capable of resolving Bragg spacings in the order of 100-1 nm, depending on sample-to-detector distance. The NanoSTAR has a variable length evacuated tube to carry X-rays from the sample to the detector, allowing both small and wide angle X-ray scattering data to be obtained from the same spot of the same sample. X-rays are generated from an electrical source using a Kristalloflex 760 X-ray generator (Bruker AXS, Germany). The X-rays are focused using cross-coupled Göbel mirrors and a 3-pinhole collimation system, to produce an X-ray beam of 0.4 mm x 0.8 mm, with a wavelength of 0.154 nm.

The detector system used by the NanoSTAR is a HI-STAR 2-dimensional detector, which consists of an X-ray proportional chamber, multiwire grid, and electronic devices used to control data collection and output. The proportional chamber consists of a beryllium window to minimize X-ray absorption, and a high-pressure xenon gas mixture. Each incoming photon becomes a charged pulse and is collected on the multiwire grid.

Diffraction profiles were taken over 3 hour exposures using a sample to detector distance of 4.5 cm, providing data in the range of 0.3 nm^{-1} to 5.3 nm^{-1}. Data were corrected for camera distortions, a background image was subtracted, and images

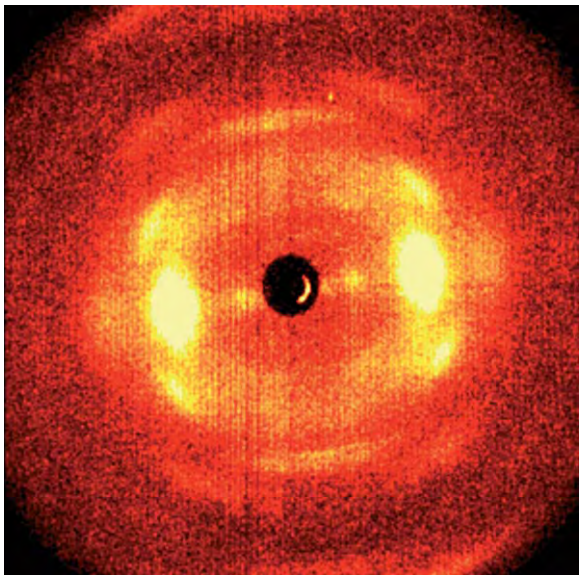

Figure 1: A wide angle X-ray diffraction image of silk. A preferred orientation is clearly observed, with the main diffraction peaks in the equatorial direction. This image covers the range of 0.29 nm^{-1} to 5.23 nm^{-1}, describing structures in the region of 3.45 nm to 0.19 nm in real space.

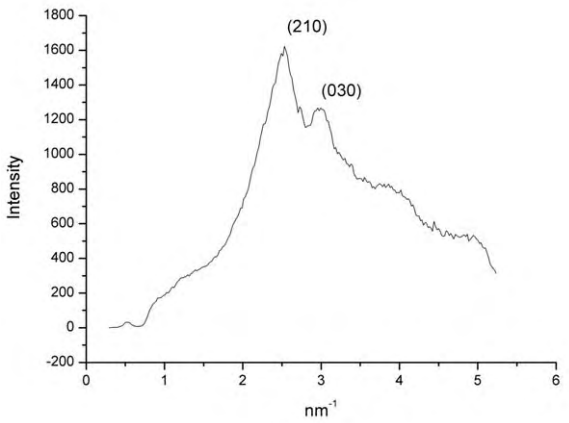

Figure 2: One dimensional linear profile from the X-ray diffraction pattern of silk. Labelled are the main observable peaks; the (210) peak of silk was used to assess the sample crystallinity and size of the crystallites.

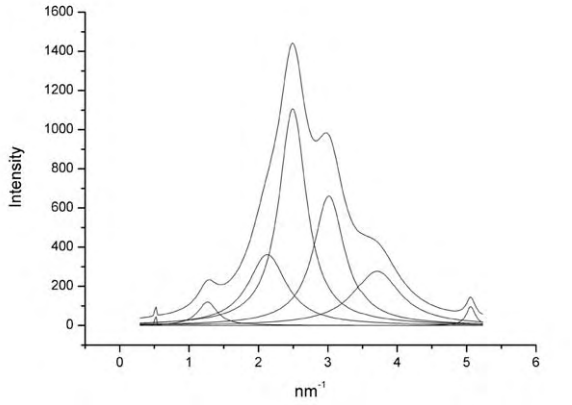

Figure 3: Peak fitting of the equatorial X-ray diffraction pattern from silk using PeakFit 4. The peak fitting was conducted to an R^2 value of over 0.98; a baseline was subtracted from the data and the peaks used for the fitting were Lorentzian in nature.

were analysed using CCP13 software. The equatorial region encompassing the main equatorial *210* reflection were taken from the two-dimensional detector output and converted to one-dimensional linear profiles for analysis. Figure 1 shows a 2-dimensional diffraction image taken from the NanoSTAR, and figure 2 displays a linear profile generated from the silk sample. The unit cell of silk (a = 0.938 nm, b = 0.949 nm, c = 0.698 nm) in which antipolar-antiparallel sheet structures exist was used to derive the Bragg peaks. Two diffraction images were taken at different locations on each sample, to ensure reproducibility.

Once one dimensional linear profiles were obtained, peaks were analysed using the program PeakFit 4 (AISN software). Images were loaded in to the program and underlying backgrounds were removed by selecting from a constant, linear, quadratic, cubic, logarithmic, exponential, power or hyperbolic function. In all cases an exponential function was selected. All observable peaks were modeled, and values such as the peak position, full width half maximum, integrated intensity, amplitude, peak contribution to the entire spectrum as a percentage, standard errors and t-values were produced in this procedure. Typical R^2 values for the peak fit ranged from 0.97 to 0.999. Figure 3 displays typical fitted peaks from silk samples. The peak profiles were examined to determine if there were any significant changes following treatments, such as the ratio of peak heights changing; none were observed.

2.3 Crystallinity Assessment

A variety of methods are available to facilitate the measurement of crystallinity from the wide angle diffraction pattern of silk, all of which include the main equatorial (*210*) reflection. Him et al[22] obtained the relative crystallinity (Xc) of cellulose samples by fitting the peaks and using the equation:

$$\mathbf{Xc = I_{200}/I_{TOT}}$$

where I_{200} is the integrated intensity of the (*200*) equatorial reflection from cellulose derived from the fitting procedure and I_{TOT} is the total integrated intensity at the position of the (*200*) reflection i.e. the sum of the peak intensity and amorphous background.

In this study, crystallinity was measured using this method, with the caveats that the Xc values are multiplied by 100 so that the crystallinity values are expressed as a percentage, and the *(210)* equatorial reflection from silk replaces the *(200)* reflection from cellulose. The integrated intensity of the peak was taken from the range of 2 nm^{-1} to 3 nm^{-1}. The crystallinity values given

are the average values taken from both measurements of each individual sample.

2.4 Crystal Size Analysis

Crystalline dimensions can be estimated from the width of peaks from wide angle diffraction patterns using the Scherrer equation[23]:

$L = 0.9\lambda/(B\cos\theta)$

Where B is the full width half maximum of the peak (in radians), λ is the X-ray wavelength (0.154 nm), and θ is the angle between incident and reflected rays. The value B was corrected for instrumental broadening of the peaks by $\sqrt{(B_1^2-B_2^2)}$, where B_1 is the width of the peak from the silk sample, and B_2 is the width of a peak taken from a sample of pure silica.

3. Results

Table 1 displays crystallinity values from the silk samples treated at 1.5 J/cm^2. A definite pattern can be discerned from the crystallinity of the silk samples: as the number of pulses increases from 4 to 16 to 64, the crystallinity of the samples is reduced. The largest reduction in most cases can be observed between 16 and 64 pulses. Laser cleaning of soiled samples produces a greater decrease in crystallinity (3.9 and 9.8% from set 3 and 4) compared to unsoiled samples (1.1 and 5.3% from sets 1 and 2).

Figure 4 displays the crystallinity versus crystal size with an increasing number of pulses following cleaning at 1.5 J/cm^2. A clear relationship can be observed: with increasing pulses the crystallinity value decreases whilst the size of the crystallites increases. This is true regardless of sample soiling.

Sample sets 2 and 4 were additionally cleaned using a range of fluence levels. Table 2 displays the crystallinity results from these samples. There is no trend displaying a reduction in crystallinity with increasing number of pulses at each fluence level, with the exception of the sample sets cleaned at 1.5 J/cm^2. However, the overall crystallinity following cleaning at this range of fluences is clear: samples treated at 0.5 J/cm^2 display higher crystallinity values than all other samples.

Sample	Xc(%)
Reference	60 ± 1
Reference	67.0 ± 0.4
Set 1, 4 pulses	63 ± 2
Set 1, 16 pulses	62.6 ± 0.3
Set 1, 64 pulses	61.6 ± 0.4
Set 2, 4 pulses	62 ± 3
Set 2, 16 pulses	62 ± 1
Set 2, 64 pulses	56.2 ± 0.9
Set 3, 4 pulses	61 ± 4
Set 3, 16 pulses	59 ± 2
Set 3, 64 pulses	57 ± 3
Set 4, 4 pulses	62.9 ± 0.6
Set 4, 16 pulses	62 ± 3
Set 4, 64 pulses	53 ± 2

Table 1: The influence of laser cleaning on the crystallinity (Xc) of silk samples. Laser cleaning was carried out at a wavelength of 532 nm and a fluence level of 1.5 J/cm^2. Sets 1 and 2 were left unsoiled; sets 3 and 4 were soiled with carbon black prior to laser cleaning. In all cases the crystallinity of the silk is reduced following exposure to a greater number of laser pulses.

Fluence (J/cm2)	Pulses	Crystallinity (%)
Unsoiled samples (set 2)		
0.5	4	67.8 ± 0.9
	16	65.4 ± 0.4
	64	67 ± 1
1	4	60 ± 2
	16	60 ± 3
	64	62 ± 3
1.5	4	61 ± 2
	16	62 ± 2
	64	56 ± 2
4.2	4	63 ± 5
	16	62 ± 1
	64	59.8 ± 0.6
Soiled samples (set 4)		
0.5	16	64.3 ± 0.6
	64	61 ± 2
1	4	65.4 ± 0.9
	16	60.3 ± 0.5
	64	65 ± 3
1.5	4	63 ± 2
	16	62 ± 2
	64	53 ± 2
4.2	4	62 ± 1
	16	61 ± 1
	64	61.0 ± 0.7

Table 2: The influence of fluence on the crystallinity of samples. Set 2 was not soiled before laser cleaning; set 4, however, was. Only samples cleaned at 1.5 J/cm^2 show a trend displaying a reduction in crystallinity with increasing number of pulses. However, the overall crystallinity following cleaning at the other fluence levels is clear: samples treated at 0.5 J/cm^2 display higher crystallinity values than the other samples.

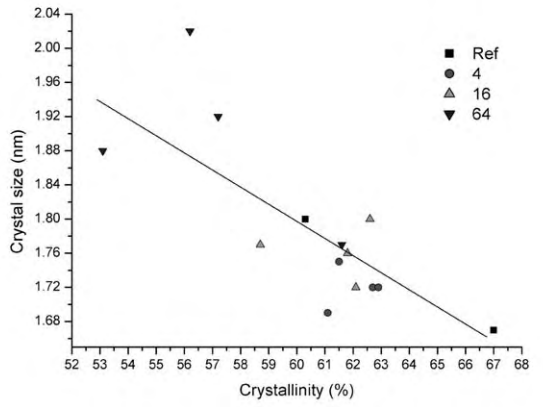

Figure 4: The relationship between crystallinity, crystal size and laser cleaning at 1.5 J/cm^2. As the number of pulses increases, from 0 through to 64, the crystallinity of the samples decreases whilst the size of the crystalline domains increases. A trendline has been added to illustrate this trend.

4. Discussion

The results displayed are an indication of a technique capable of providing sensitive information regarding the crystallinity of samples following treatments. One main benefit of employing the NanoSTAR is that it provides a robust and stable means of measuring the diffraction properties of a number of samples in one experiment. Although taking one X-ray diffraction image on the NanoSTAR takes longer than it would at a synchrotron radiation source (typically 3 hours versus 3 minutes at SRS Daresbury, UK, or 0.3 seconds at ESRF, Grenoble, France), the NanoSTAR can operate continuously without supervision, allowing a large bank of data to be collected. At synchrotron radiation sources, the beamtime allowed for experiments is extremely limited, and must be applied for months in advance. In addition, the NanoSTAR boasts an X-Y movable sample chamber, allowing multiple samples to be analysed at a number of locations per sample. Results are produced from the NanoSTAR and analysed quickly, allowing a large set of samples to be assessed in a short space of time.

One major benefit of X-ray diffraction as a sensitive analytical technique is that it is intrinsically non-destructive to the samples in question as X-rays interact weakly with matter. However, the experimental set-up on the NanoSTAR, where the samples are placed in a vacuum for several hours, may induce some damage to the samples by way of dehydration. For central synchrotron radiation facilities such as SRS Daresbury, UK, the European Synchrotron Radiation Facility, Grenoble, France or the new DIAMOND facility, due to open shortly in the UK, where samples can be analysed in air, valuable documents or materials can be analysed and returned to their owners intact, without the need for cutting or drilling the samples. Alternatively, samples used in X-ray diffraction experiments can be utilised for destructive analysis by other techniques, allowing data from different sources to be available from the same area of the same sample.

The crystallinity of the samples was the main focus of the work presented here. The measurement of crystallinity has developed mainly for cellulose and paper samples, although the technique can be adapted for silk. One way of measuring the crystallinity from diffraction patterns is to measure the minima and maxima of the curve above the base line [24]. Segal *et al* [25] sampled the height of the main equatorial reflection of cellulose and compared that to a region with no diffraction peaks present to produce a crystallinity index. Foner & Adan[26] applied Segal's method specifically to paper samples. It should be noted that these articles use the (*002*) reflection to assess cellulose crystallinity; this is due to the unit cell nomenclature of the time[27]. What was termed the (*002*) reflection is now termed the (*200*) equatorial reflection. Another method to assess crystallinity is to use the integrated intensity of the (*200*) reflection[28-30]. Him et al[22] adapted this technique to incorporate computational analyses of the integrated intensity of the (*200*) peak, and the method used in this study is derived from this.

X-ray diffraction has been used to study the effects of laser cleaning a number of cultural heritage artifacts including parchment[6,7], marble[31,32], bone[33] and pigments[34,35].

In this study laser cleaning of silk was investigated. von Lerber et al[12], using a variety of techniques including viscometry, colorimetry and polarised Fourier transform spectroscopy (pol-FTIR) suggested that upon laser cleaning chemical changes such as chain scission were occurring. This is in agreement with the reduction in crystallinity seen here. As the long polymer chains undergo scission, they become more likely to assume conformations other than a crystalline one. Thus, were laser cleaning to carry on for an excessive period of time, it is conceivable that the crystalline character of the silk may be lost altogether.

An interesting feature of these results is the relationship between crystal size and crystallinity. As the crystallinity decreases, the crystal size increases. One speculative explanation is that upon laser cleaning, the crystallites present may undergo a conformational change, with a number of chains assuming a more random conformation. Such chains would not contribute to the crystalline part of the diffraction profile, and may cause an expansion of the crystallite size. This would, in part, explain the behaviour of the crystal size and crystallinity upon laser cleaning, although other explanations may also be possible.

The effect of fluence level on the crystallinity of the samples is of interest. For sample set 2, which was not soiled, cleaning at 0.5 J/cm^2 produced crystallinity values in the range of 65-68%, reducing to 59-63% following cleaning at 4.2 J/cm^2. Sample set 4 was soiled with carbon black before cleaning, and displayed crystallinity values of 61-64% following cleaning at 0.5 J/cm^2, reducing to 61-62% following cleaning at 4.2 J/cm^2. This suggests that at low fluence levels the addition of carbon black to the samples before cleaning further damages the silk structure relative to a sample not soiled with carbon black. von Lerber et al[12] also noted that samples that had been soiled before cleaning displayed more pronounced changes in terms if their physical and

chemical characteristics; this is in agreement with the assessment conducted here.

5. Conclusion

X-ray diffraction is a sensitive, non-destructive tool capable of providing detailed structural information regarding a sample. The examples used in this case were laser cleaned silk samples. The results of this analysis were dependent on two factors: number of pulses and laser fluence. At a fluence level of 1.5 J/cm^2, an increasing number of pulses caused a reduction in crystallinity, and an increase in crystal size. As fluence levels were increased beyond 0.5 J/cm^2, overall crystallinity was reduced.

Acknowledgements

Thanks to Dr. Matija Strlič, University of Ljubljana, and Dr. Jana Kolar, National and University Library, Ljubljana for useful discussions and advice. Thanks to Clark Maxwell, Cardiff University, for technical assistance and advice using the NanoSTAR. CCP13 software was used in the data reduction steps of this analysis.

References

1. A. Costela, I. Garcia-Moreno, C. Gomez, O. Caballero, R. Sastre, *Cleaning graffitis on urban buildings by use of second and third harmonic wavelength of a Nd : YAG laser: a comparative study*. App. Surf. Sci., 2003, **207**, 86-99.

2. S. Siano, R. Salimbeni, *The gate of paradise: physical optimization of the laser cleaning approach*, Studies in Conservation, 2001, **46**, 269-281.

3. M. Cooper, *Laser Cleaning in Conservation*, Butterworth Heinemann, Oxford, UK, 1997.

4. M. I. Cooper, D. C. Emmony, J. Larson, *Characterisation of laser cleaning of limestone*, Opt. Laser Technol., 1995, **27**, 69-73.

5. J. F. Asmus, M. Seracini, M. J. Zetler, *Surface morphology of laser-cleaned stone*, Lithoclastia, 1976, **1**, 23-45.

6. C. J. Kennedy, J. C. Hiller, D. Lammie, M. Drakopoulos, M. Vest., M. Cooper, W. P. Adderley, T. J. Wess, *Microfocus X-ray diffraction of historical parchment reveals variations in structural features through parchment cross sections*, Nano Lett., 2004, **4**, 1373-1380.

7. C. J. Kennedy, M. Vest, M. Cooper, T. J. Wess, *Laser cleaning of parchment: structural, thermal and biochemical studies into the effect of wavelength and fluence*, App. Surf. Sci., 2004, **227**, 151-163.

8. W. Kautek, S. Pentzien, A. Conradi, D. Leichtfried, L. Puchinger, *Diagnostics of parchment laser cleaning in the near-ultraviolet and near-infrared wavelength range: a systematic scanning electron microscopy study*, J. Cult. Herit., 2003, **4**, 179s-184s.

9. M. Strlič, J. Kolar, V.-S. Šelih, *Marinček, M. Surface modification during Nd:YAG (1064 nm) pulsed laser cleaning of organic fibrous materials*, App. Surf. Sci., 2003, **207**, 236-245.

10. J. Kolar, M. Strlič, D. Muller-Hess, A. Gruber, K. Troschke, S. Pentzien, W. Kautek, *Laser cleaning of paper using Nd:YAG laser running at 532 nm,* J. Cult. Herit., 2003, **4,** s1, 185-187.

11. W. Kautek, S. Pentzien, P. Rudolph, J. Kruger, E. Konig, *Laser interaction with coated collagen and cellulose fibre composites: fundamentals of laser cleaning of ancient parchment manuscripts and paper,* App. Surf. Sci, 1998, **127-129**, 746-754.

12. K. von Lerber, S. Pentzien, M. Strlič, W. Kautek, *Laser cleaning of silk – a first systematic evaluation,* Preprints of the 14th Triennial ICOM-CC Meeting, The Hague, The Netherlands, 2005, vol.II, 978-988.

13. J. Schroeter, F. Felix, *Melting cellulose*, Cellulose, 2005, **12**, 159-165.

14. N. Y. Ignatieva, V. V. Lunin, S. V. Averkiev, A. F. Maiorova, V. N. Bagratashvili, E. N. Sobol, *DSC investigation of connective tissues treated by IR-laser radiation*, Thermochim. Acta, 2004, **422**, 43-48.

15. Y. Tsuboi, H. Adachi, K. Yamada, H. Miyasaka, A. Itaya, *Laser ablation of silk protein (fibroin) films,* Jpn. J. Appl. Phys., 2002, **41**, 4772-4779.

16. R. M. Miranda, *Structural analysis of the heat affected zone of marble and limestone tiles cut by CO_2 laser*, Mater. Charact., 2004, **53**, 411-417.

17. M. Burghammer, M. Muller, C. Riekel, *X-ray synchrotron radiation microdiffraction on fibrous biopolymers like cellulose and in particular spider silks*, Recent Res. Devel. Macromol., 2003, **7**, 103-125.

18. C. Riekel, *Applications of micro-SAXS/WAXS to study polymer fibers*, Nucl. Instrum. Meth. B, 2003, **199**, 106-111.

19. R. W. Work, P. D. Emerson, *An apparatus and technique for the forcible silking of spiders,* J. Arachnol., 1982, **10**, 1–10.

20. C. Riekel, C. Bränden, C. Craig, C. Ferrero, F. Heidelbach, M. Müller, *Aspects of X-ray diffraction on single spider fibers,* Int. J. Biol. Macromol*,* 1999, **24**, 179-186.

21. T. J. Wess, M. Drakopoulos, A. Snigirev, J. Wouters, O, Paris, P. Fratzl, M. Collins, J. Hiller, K. Nielsen, *The use of small angle X-ray diffraction studies for the analysis of structural features in archaeological samples*, Archaeomerty, 2001, **43**, 117-129.

22. J. L. K. Him, H. Chanzy, M. Müller, J-L Putaux, T. Imai, V. Bulone, *In Vitro Versus in Vivo cellulose microfibrils from plant primary wall synthases: structural differences,* J. Biol. Chem., 2002, **277**, 36931-36939.

23. H. P. Klug, L. E. *Alexander, X-ray diffraction procedures for polycrystalline and amorphous materials,* Wiley, New York, 1954, 491-538.

24. G. L. Clark, H. C. Telford, *Quantatative X-ray determination of amorphous phase in wood pulps as related to physical and chemical properties*, Anal. Chem., 1955, **27**, 888-895.

25. L. Segal, J. J. Creely, Jr. A. E. Martin, C. M. Conrad, *An empirical method for estimating the degree of crystallinity of native cellulose using the X-ray diffractometer*, Text. Res. J., 1959, **29,** 786-794.

26. H. A. Foner, N. Adan, *The characterisation of papers by X-ray diffraction (XRD): measurement of cellulose crystallinity and determination of mineral composition*, J. Forensic Sci. Soc., 1983, **23**, 313-321.

27. P. Zugenmaier, Conformation *and packing of various crystalline cellulose fibers*, Prog. Polym. Sci., 2001, **26,** 1341-1417.

28. P. H. Herman, A. Weidlinger, Quantatative X-ray investigations on the crystallinity of cellulose fibres, *J. Appl. Phys,* 1948, **19**, 491-506.

29. S. Krimm, A. V. Tobolsky, *Quantatative X-ray studies of order in amorphous and crystalline polymers*, J. Polym. Sci*,* 1951-2, **1**, 57-76.

30. J. B. Nichols, *X-ray and infra-red studies on the extent of*

crystallization of polymers, J. Appl. Phys., 1954, **25**, 840-847.

31. C. Rodriguez-Navarro, A. Rodriguez-Navarro, K. Elert, E. Sebastian, *Role of marble microstructure in near-infrared laser-induced damage during laser cleaning.* J. Appl. Phys., 2004, **95**, 3350-3357.

32. P. Pouli, V. Zafiropulos, C. Balas, Y. Doganis, A. Galanos, *Laser cleaning of inorganic encrustation on excavated objects: evaluation of the cleaning result by means of multi-spectral imaging,* J. Cult. Herit., 2003, **4**, s1, 338-342.

33. F. Landucci, R. Pini, S. Siano, R. Salimbeni, E. Pecchioni, *Laser cleaning of fossil vertebrates: a preliminary report,* J. Cult. Herit., 2000, **1**, s1, S263-S267.

34. R. J. Gordon Sobbot, T. Heinze, K. Neumeister, J. Hildenhagen, *Laser interaction with polychromy: laboratory investigations and on-site observations,* J. Cult. Herit., 2003, **4**, s1, 276-286.

35. M. I. Cooper, P. S. Fowles, C. C. Tang, *Analysis of the laser-induced discoloration of lead white pigment*, Appl. Surf. Sci., 2002, **201**, 75-84.